

Supplementary Material 1: Conceptual ECH<sub>2</sub>O-iso energy and water balance

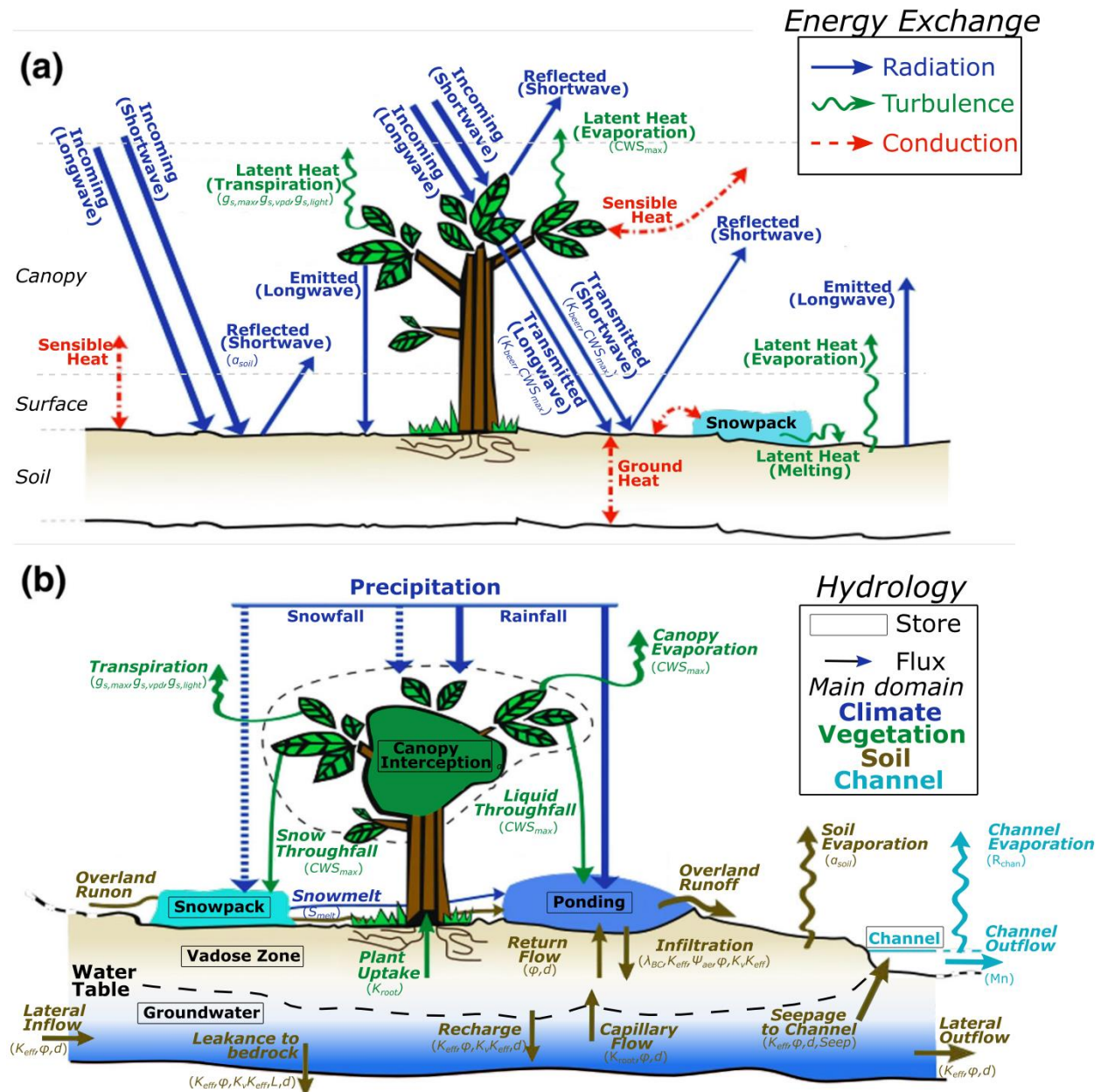
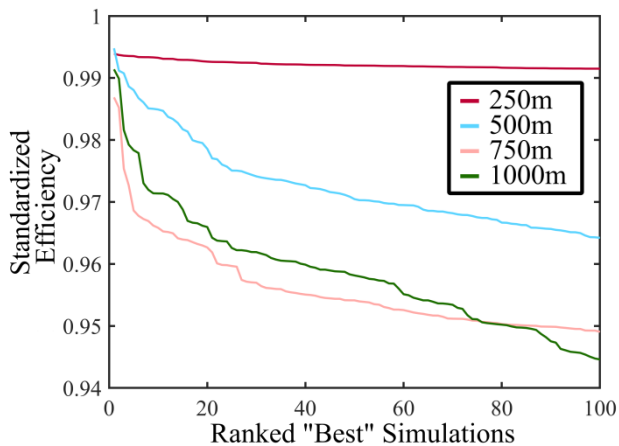


Figure S1: Conceptual framework of the energy and water balance storages and fluxes in the ECH<sub>2</sub>O (-iso) model. Parentheses below fluxes indicate parameters directly controlling each flux (adapted from Douinot et al. (2019)).

## Supplementary Material 2: Multicriteria calibration, parameterisation, and validation

Calibration was conducted using multicriteria calibration using fluxes, discharge, and isotopes (Table 1). Due to the large discrepancies in the number of samples of calibration data (e.g. 8-day data for the whole time-period vs. weekly stream isotope data for 2 two years), the empirical cumulative distributions (eCDF) were inversely weighted by the number of samples (e.g. additional weighting given to isotopic simulations relative to discharge). A threshold quantile for the weighted eCDF was determined for each model resolution to produce exactly 100 parameter sets (Ala-aho et al., 2017). Due to the use of eCDFs, the overall efficiency ranges between 0 and 1, where a value of 1 indicates that all output from a given simulation is the best-observed model efficiency from all parameter sets. A value of 1 does not indicate that there is a perfect fit (e.g. may have Nash-Sutcliffe efficiency of 0.7 for discharge). Since trade-offs generally occur within multicriteria calibration (e.g. Boyle et al. (2000)), a value of 1 is not expected from any calibration. The values of overall efficiency indicate the threshold value, for example, 0.95 indicates the overall parameter sets were in the top 5% for all model output.



**Figure S2: The standardized weighted multicriteria efficiency of each model scale, standardized against the best simulations of the given scale (100,000 simulations) and shown for the 100 “best” simulations.**

- 20 Simulations in the finer resolution (250 and 500 m) show higher overall efficiency sustained for the 100 best simulations (Fig. S2). There is a very limited decrease in model performance for 250m in the 100 best simulations compared to the other resolutions which had a much more rapid decrease in overall model performance with from the best to 100th best parameter set. There was a limited difference in the 750 and 1000m model resolutions for the rate of decrease in model performance (Fig. S2).
- 25 The overall best model performance is dependent on the best possible model efficiency of output for each resolution. Changing the model resolution independently changes the model efficiency (Table S1). In general, discharge, isotopes (stream, soil, and groundwater) have better possible model efficiency at finer resolutions, as indicated with the “Best Fit” (Table S1). Latent heat and evapotranspiration, calibrated against remotely sensed data (MODIS), showed higher possible

30 efficiency with coarser resolutions. Soil moisture simulations were inconsistent for both remote data sources (ERA5) or field measurements, and were more dependent on the site (e.g. Forest A was better at coarser resolutions, Table S1).

**Table S1: Best efficiency criteria for each model scale under single criteria calibration (i.e. best possible value for an output).**

		250m	500m	750m	1000m	Best Fit
<b>Discharge</b>	<b>Demnitz Mill</b>	0.820	0.806	0.760	0.809	250m
	<b>Demnitz</b>	0.702	0.744	0.660	0.643	500m
<b>Isotopes</b>	<b>Peat North</b>	0.011	0.010	0.010	0.010	500m
	<b>Peat South</b>	0.014	0.016	0.020	0.018	250m
	<b>Bruchmill</b>	0.018	0.020	0.020	0.024	250m
	<b>Demnitz Mill</b>	0.023	0.024	0.023	0.025	750m
<b>ET</b>	<b>Conifers</b>	0.699	0.718	0.723	0.737	1000m
	<b>Croplands</b>	0.745	0.687	0.707	0.726	250m
	<b>Forest A</b>	0.744	0.663	0.756	0.766	1000m
<b>Transpiration</b>	<b>Forest A</b>	0.777	0.875	0.792	0.878	250m
<b>Latent Heat</b>	<b>Conifers</b>	0.705	0.732	0.727	0.734	1000m
	<b>Croplands</b>	0.583	0.548	0.555	0.641	1000m
	<b>Forest A</b>	0.624	0.568	0.681	0.668	750m
<b>Soil Moisture (ERA 5)</b>	<b>Alt Madlitz</b>	0.720	0.627	0.657	0.650	250m
	<b>Forest A</b>	0.696	0.663	0.713	0.732	1000m
<b>Soil Moisture (Measured)</b>	<b>Alt Madlitz</b>	0.729	0.663	0.661	0.660	250m
	<b>Forest A</b>	0.873	0.828	0.882	0.880	750m
<b>Soil Isotopes</b>	<b>Forest A</b>	0.066	0.073	0.068	0.082	250m
<b>Groundwater Isotopes</b>	<b>GW 4</b>	0.006	0.006	0.009	0.014	250m
	<b>GW 8</b>	0.014	0.014	0.014	0.014	1000m

The posterior 75th and 25th parameter quantiles for each calibrated soil, vegetation, and channel (Table S2), and median parameter values (Fig. S3) show the distribution of calibrated parameters for each model resolution.

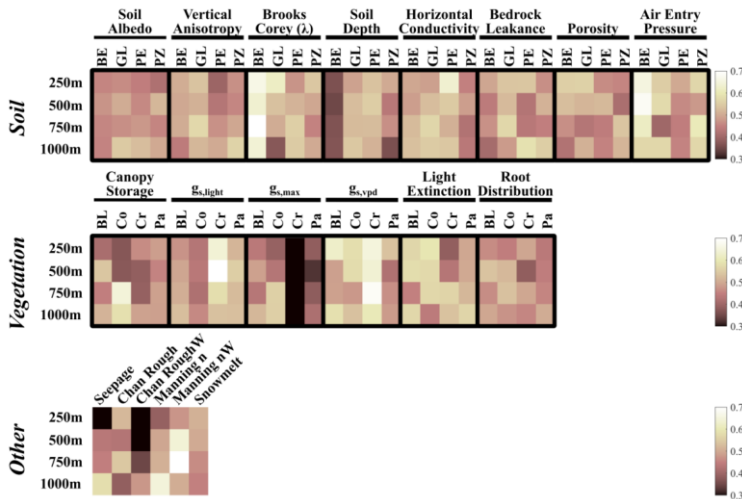


**Figure S3: Median parameter value standardized from the maximum parameter range for all calibrated parameters in the soil, vegetation, and non-soil or vegetation dependent parameters.**

Fig. S3 shows the median calibrated parameter value, normalized on a scale between 0 (lowest value of parameter range) and 1 (highest value of parameter range). Darker colours indicate a skew of the calibrated parameters towards lower parameter values and lighter colours indicate a skew of calibrated parameters towards higher parameter values. The scales showed relatively limited differences for most parameters. Some parameter distributions shifts were similar across all model resolution, notably shallower soil depth and higher Brook-Corey lambda in brown earth (Fig. S3). The most sensitive parameters (e.g. anisotropy, conductivity, Manning's n, leakance, seepage) showed relatively smooth changes with model resolution. Particularly with finer resolutions, anisotropy (higher in BE and lower in PE and PZ), hydraulic conductivity (lower in BE, GL, PE), manning's n (lower), and seepage of groundwater into the channels (decreasing).

**Table S2: The 75th and 25th percentiles of posterior parameter ranges for soil parameters (brown earth, gley, peat, and podzol, BE, GL, PE, and PZ, respectively), vegetation parameters (croplands, broadleaf, conifers, and pasturelands, Cr, BL, Co, and Pa, respectively), and channel parameters for each model scale (250, 500, 750, and 1000m). Percentages in parentheses indicate the percent change of the interquartile range from the a priori parameter range.**

		Soil			
		250m	500m	750m	1000m
Soil Albedo	BE	0.18 - 0.12 (18 %)	0.17 - 0.13 (-22 %)	0.18 - 0.13 (0 %)	0.18 - 0.13 (0 %)
	GL	0.18 - 0.12 (18 %)	0.17 - 0.13 (-22 %)	0.17 - 0.12 (0 %)	0.17 - 0.12 (0 %)
	PE	0.18 - 0.13 (0 %)	0.18 - 0.13 (0 %)	0.17 - 0.13 (-22 %)	0.17 - 0.12 (0 %)
	PZ	0.18 - 0.13 (0 %)	0.17 - 0.13 (-22 %)	0.18 - 0.13 (0 %)	0.17 - 0.13 (-22 %)
Vertical Aniso.	BE	0.31 - 0.13 (-5 %)	0.28 - 0.12 (-17 %)	0.30 - 0.10 (5 %)	0.29 - 0.09 (5 %)
	GL	0.31 - 0.10 (10 %)	0.33 - 0.11 (15 %)	0.30 - 0.08 (15 %)	0.29 - 0.10 (0 %)
	PE	0.32 - 0.13 (0 %)	0.32 - 0.14 (-5 %)	0.31 - 0.12 (0 %)	0.30 - 0.08 (15 %)
	PZ	0.30 - 0.11 (0 %)	0.30 - 0.12 (-5 %)	0.29 - 0.11 (-5 %)	0.30 - 0.11 (0 %)
Brooks Corey	BE	5.46 - 3.16 (2 %)	5.15 - 3.26 (-17 %)	5.00 - 3.13 (-18 %)	5.51 - 3.20 (3 %)
	GL	5.48 - 3.54 (-15 %)	5.68 - 3.69 (-12 %)	6.13 - 3.82 (3 %)	6.26 - 4.02 (0 %)
	PE	12.47 - 5.53 (7 %)	11.68 - 5.21 (0 %)	12.4 - 4.82 (15 %)	11.74 - 5.04 (3 %)
	PZ	5.31 - 3.35 (-4 %)	5.28 - 3.65 (-23 %)	5.61 - 3.37 (9 %)	5.51 - 3.40 (3 %)
Soil Depth	BE	7.67 - 4.09 (-17 %)	7.5 - 4.27 (-27 %)	7.58 - 3.84 (-13 %)	7.67 - 3.71 (-7 %)
	GL	7.27 - 2.17 (18 %)	6.65 - 2.7 (-7 %)	7.02 - 2.10 (15 %)	7.12 - 2.40 (10 %)
	PE	6.65 - 2.84 (-11 %)	6.99 - 2.49 (6 %)	6.60 - 2.32 (1 %)	7.02 - 2.47 (7 %)
	PZ	6.77 - 2.58 (-1 %)	7.75 - 2.94 (12 %)	7.55 - 2.84 (10 %)	7.35 - 3.22 (-3 %)
Horiz. Cond.	BE	$1.92 \times 10^{-3}$ - $1.30 \times 10^{-4}$ (-72 %)	$1.59 \times 10^{-3}$ - $4.00 \times 10^{-5}$ (-46 %)	$2.11 \times 10^{-3}$ - $1.00 \times 10^{-5}$ (-10 %)	$1.25 \times 10^{-3}$ - $1.00 \times 10^{-5}$ (-10 %)
	GL	$6.24 \times 10^{-3}$ - $2.00 \times 10^{-5}$ (0 %)	$4.41 \times 10^{-3}$ - $1.00 \times 10^{-5}$ (-1 %)	$3.58 \times 10^{-3}$ - $1.00 \times 10^{-5}$ (1 %)	$4.00 \times 10^{-3}$ - $1.00 \times 10^{-5}$ (1 %)
	PE	$1.55 \times 10^{-3}$ - $1.00 \times 10^{-5}$ (-13 %)	$3.82 \times 10^{-3}$ - $1.00 \times 10^{-5}$ (1 %)	$2.78 \times 10^{-3}$ - $3.00 \times 10^{-5}$ (-20 %)	$4.88 \times 10^{-3}$ - $1.00 \times 10^{-5}$ (-20 %)
	PZ	$5.77 \times 10^{-3}$ - $2.00 \times 10^{-5}$ (0 %)	$8.06 \times 10^{-3}$ - $1.00 \times 10^{-5}$ (13 %)	$6.88 \times 10^{-3}$ - $2.00 \times 10^{-5}$ (5 %)	$1.26 \times 10^{-2}$ - $3.00 \times 10^{-5}$ (5 %)
Leak	BE	$1.06 \times 10^{-6}$ - $5.60 \times 10^{-9}$ (-28 %)	$2.90 \times 10^{-6}$ - $6.00 \times 10^{-9}$ (-11%)	$3.34 \times 10^{-6}$ - $2.40 \times 10^{-9}$ (5 %)	$7.63 \times 10^{-6}$ - $6.30 \times 10^{-9}$ (5 %)
	GL	$5.71 \times 10^{-6}$ - $2.60 \times 10^{-9}$ (11 %)	$4.57 \times 10^{-6}$ - $6.20 \times 10^{-9}$ (-5 %)	$2.23 \times 10^{-6}$ - $4.10 \times 10^{-9}$ (-9 %)	$1.82 \times 10^{-6}$ - $3.10 \times 10^{-9}$ (-9 %)
	PE	$3.43 \times 10^{-6}$ - $1.50 \times 10^{-9}$ (12 %)	$6.46 \times 10^{-6}$ - $2.90 \times 10^{-9}$ (11 %)	$5.63 \times 10^{-6}$ - $5.30 \times 10^{-9}$ (1 %)	$2.75 \times 10^{-6}$ - $3.30 \times 10^{-9}$ (1 %)
	PZ	$6.25 \times 10^{-6}$ - $6.30 \times 10^{-9}$ (0 %)	$2.55 \times 10^{-6}$ - $6.40 \times 10^{-9}$ (-14%)	$4.95 \times 10^{-6}$ - $3.40 \times 10^{-9}$ (5 %)	$5.55 \times 10^{-7}$ - $4.60 \times 10^{-9}$ (5 %)

<b>Porosity</b>	BE	0.48 - 0.37 (10 %)	0.46 - 0.38 (-22 %)	0.48 - 0.38 (0 %)	0.50 - 0.41 (-11 %)
	GL	0.47 - 0.35 (18 %)	0.47 - 0.37 (0 %)	0.48 - 0.40 (-22 %)	0.46 - 0.36 (0 %)
	PE	0.60 - 0.45 (-24 %)	0.63 - 0.43 (5 %)	0.63 - 0.43 (5 %)	0.61 - 0.41 (5 %)
	PZ	0.48 - 0.36 (29 %)	0.46 - 0.38 (-12 %)	0.46 - 0.37 (0 %)	0.46 - 0.37 (0 %)
<b>Entry Pressure</b>	BE	0.32 - 0.14 (-36 %)	0.33 - 0.12 (-21 %)	0.35 - 0.14 (-21 %)	0.40 - 0.15 (-4 %)
	GL	0.33 - 0.13 (-5 %)	0.34 - 0.14 (-5 %)	0.39 - 0.20 (-10 %)	0.32 - 0.17 (-33 %)
	PE	0.89 - 0.30 (3 %)	0.95 - 0.34 (7 %)	0.89 - 0.41 (-17 %)	0.92 - 0.32 (5 %)
	PZ	0.29 - 0.11 (18 %)	0.30 - 0.15 (0 %)	0.26 - 0.10 (6 %)	0.28 - 0.1 (18 %)
<b>Seep.</b>	All	1.72 - 0.17 (-85 %)	0.58 - 0.02 (-53 %)	0.50 - 0.02 (-49 %)	0.18 - 0.01 (-41 %)
<b>Snow melt Coeff.</b>	All	$1.5 \times 10^{-7} - 6.0 \times 10^{-8}$ (-46 %)	$1.7 \times 10^{-7} - 6.0 \times 10^{-8}$ (-44 %)	$1.6 \times 10^{-7} - 6.0 \times 10^{-8}$ (-41 %)	$1.6 \times 10^{-7} - 7.0 \times 10^{-8}$ (-62 %)
<b>Vegetation</b>					
		<b>250m</b>	<b>500m</b>	<b>750m</b>	<b>1000m</b>
<b>Canopy Storage</b>	Cr	$2.8 \times 10^{-4} - 1.5 \times 10^{-4}$ (-98 %)	$3.1 \times 10^{-4} - 1.5 \times 10^{-4}$ (-87 %)	$2.9 \times 10^{-4} - 1.7 \times 10^{-4}$ (-114 %)	$2.9 \times 10^{-4} - 1.5 \times 10^{-4}$ (-97 %)
	BL	$2.8 \times 10^{-3} - 5.8 \times 10^{-4}$ (-8 %)	$2.3 \times 10^{-3} - 4.6 \times 10^{-4}$ (-4 %)	$3.2 \times 10^{-3} - 5.8 \times 10^{-4}$ (1 %)	$2.3 \times 10^{-3} - 4.1 \times 10^{-4}$ (2 %)
	Co	$3.3 \times 10^{-3} - 6.1 \times 10^{-4}$ (-1 %)	$3.8 \times 10^{-3} - 5.2 \times 10^{-4}$ (15 %)	$2.0 \times 10^{-3} - 3.5 \times 10^{-4}$ (2 %)	$2.1 \times 10^{-3} - 3.6 \times 10^{-4}$ (5 %)
	Pa	$2.9 \times 10^{-4} - 1.5 \times 10^{-4}$ (-90 %)	$3.0 \times 10^{-4} - 1.4 \times 10^{-4}$ (-86 %)	$3.1 \times 10^{-4} - 1.4 \times 10^{-4}$ (-80 %)	$3.0 \times 10^{-4} - 1.4 \times 10^{-4}$ (-81 %)
<b>g<sub>light</sub></b>	Cr	310 - 83 (-9 %)	299 - 45 (2 %)	341 - 86 (2 %)	361 - 98 (5 %)
	BL	399 - 132 (6 %)	359 - 135 (-11 %)	358 - 129 (-9 %)	366 - 126 (-4 %)
	Co	405 - 146 (4 %)	370 - 129 (-4 %)	388 - 153 (-6 %)	384 - 128 (3 %)
	Pa	345 - 132 (-16 %)	365 - 144 (-12 %)	339 - 70 (7 %)	322 - 65 (3 %)
<b>g<sub>s,max</sub></b>	Cr	$2.32 \times 10^{-2} - 1.28 \times 10^{-2}$ (-97 %)	$2.23 \times 10^{-2} - 1.11 \times 10^{-2}$ (-81 %)	$2.27 \times 10^{-2} - 1.05 \times 10^{-2}$ (-75 %)	$2.34 \times 10^{-2} - 1.30 \times 10^{-2}$ (-97 %)
	BL	$6.40 \times 10^{-3} - 2.10 \times 10^{-3}$ (-4 %)	$6.55 \times 10^{-3} - 1.96 \times 10^{-3}$ (5 %)	$5.63 \times 10^{-3} - 2.04 \times 10^{-3}$ (-13%)	$5.97 \times 10^{-3} - 2.04 \times 10^{-3}$ (-7 %)
	Co	$7.10 \times 10^{-3} - 2.00 \times 10^{-3}$ (8 %)	$6.28 \times 10^{-3} - 1.91 \times 10^{-3}$ (3 %)	$5.59 \times 10^{-3} - 1.86 \times 10^{-3}$ (-4 %)	$4.67 \times 10^{-3} - 1.56 \times 10^{-3}$ (-5 %)
	Pa	$6.00 \times 10^{-3} - 1.6 \times 10^{-3}$ (-14 %)	$7.80 \times 10^{-3} - 1.31 \times 10^{-3}$ (18 %)	$6.39 \times 10^{-3} - 1.25 \times 10^{-3}$ (8 %)	$6.68 \times 10^{-3} - 1.23 \times 10^{-3}$ (12 %)
<b>g<sub>s,vpd</sub></b>	Cr	$1.5 \times 10^{-4} - 1 \times 10^{-5}$ (-34 %)	$1.5 \times 10^{-4} - 1.0 \times 10^{-5}$ (-33 %)	$9.0 \times 10^{-5} - 1.0 \times 10^{-6}$ (-42 %)	$1.8 \times 10^{-4} - 1.0 \times 10^{-5}$ (-34 %)
	BL	$4.0 \times 10^{-4} - 1.0 \times 10^{-5}$ (-11 %)	$1.9 \times 10^{-3} - 0.00002$ (4 %)	$1.0 \times 10^{-3} - 1.0 \times 10^{-5}$ (3 %)	$5.7 \times 10^{-4} - 1 \times 10^{-5}$ (-11 %)
	Co	$4.5 \times 10^{-4} - 1.0 \times 10^{-5}$ (-13 %)	$7.3 \times 10^{-4} - 1.0 \times 10^{-5}$ (-17 %)	$6.6 \times 10^{-4} - 1.0 \times 10^{-5}$ (2 %)	$5.0 \times 10^{-4} - 1 \times 10^{-5}$ (-27 %)
	Pa	$3.7 \times 10^{-4} - 1.0 \times 10^{-5}$ (-33 %)	$1.4 \times 10^{-3} - 2.0 \times 10^{-5}$ (-9 %)	$5.5 \times 10^{-4} - 1.0 \times 10^{-5}$ (-13 %)	$1.4 \times 10^{-3} - 1.0 \times 10^{-5}$ (6 %)
<b>Light Extinction</b>	Cr	0.64 - 0.50 (-7 %)	0.63 - 0.50 (-14 %)	0.61 - 0.49 (-22 %)	0.62 - 0.47 (0 %)
	BL	0.62 - 0.46 (6 %)	0.60 - 0.46 (-7 %)	0.61 - 0.48 (-14 %)	0.62 - 0.46 (6 %)
	Co	0.61 - 0.46 (0 %)	0.62 - 0.48 (-7 %)	0.62 - 0.48 (-7 %)	0.64 - 0.49 (0 %)
	Pa	0.61 - 0.49 (-22 %)	0.63 - 0.50 (-14 %)	0.63 - 0.47 (6 %)	0.60 - 0.47 (-14 %)
<b>Root Distribution</b>	Cr	7.60 - 3.50 (-18 %)	7.91 - 4.01 (-24 %)	6.94 - 3.38 (-33 %)	7.75 - 3.60 (-18 %)
	BL	3.70 - 1.40 (-5 %)	3.59 - 1.29 (-6 %)	3.78 - 1.25 (3 %)	3.69 - 1.77 (-24 %)
	Co	4.00 - 1.50 (4 %)	3.85 - 1.43 (-1 %)	3.49 - 1.26 (-9 %)	4.02 - 1.39 (7 %)
	Pa	7.70 - 2.80 (-1 %)	7.42 - 3.26 (-17 %)	7.83 - 3.61 (-16 %)	7.30 - 2.80 (-10 %)
<b>Channel Parameters</b>					
		<b>250m</b>	<b>500m</b>	<b>750m</b>	<b>1000m</b>

<b>Chan Rough</b>	24.72 - 15.46 (-8 %)	26.47 - 15.2 (12 %)	25.31 - 15.56 (-3 %)	26.86 - 15.78 (10 %)
<b>Chan Rough(W)</b>	13.74 - 10.07 (-31 %)	14.07 - 10.47 (-33 %)	13.41 - 9.31 (-20 %)	12.56 - 7.75 (-4 %)
<b>Manning n</b>	0.03 - 0.02 (0 %)	0.03 - 0.02 (0 %)	0.03 - 0.02 (0 %)	0.03 - 0.01 (67 %)
<b>Manning n (W)</b>	0.39 - 0.18 (-17 %)	0.37 - 0.04 (28 %)	0.26 - 0.06 (-22 %)	0.40 - 0.04 (36 %)

Model validation was conducted for the average flow years observed from 2015 – 2017. The data available for validation were not as robust as the calibration period because isotopic measurement didn't begin until 2018. Due to the severe drought in the catchment during 2018 (Smith et al., 2020;Kleine et al., 2020), stream, soil, and groundwater isotopes were not representative for validation, and 2019 isotopic data were required for calibration (calibration during a non-extreme drought). The trend of increasing efficiency with coarser model resolutions during validation are similar to the calibration (Table 4). Similarly, soil moisture, which showed higher efficiency for finer resolutions, showed higher efficiency for finer resolutions during validation. Discharge efficiency during validation was somewhat anomalous, with a lower efficiency at 250m than at coarser scales, contrary to the higher efficiency at finer resolutions in calibration.

60 **Table S3: Median efficiency for the validation period 2015 – 2017 for discharge, evapotranspiration, latent heat, and soil moisture**

		<b>250m</b>	<b>500m</b>	<b>750m</b>	<b>1000m</b>
<b>Discharge</b>	<b>Demnitz Mill</b>	0.35	0.36	0.43	0.44
<b>Evapo-transpiration</b>	<b>Forest</b>	0.52	0.48	0.60	0.61
	<b>Alt Madlitz</b>	0.47	0.45	0.49	0.53
	<b>Conifer</b>	0.02	0.25	0.33	0.23
<b>Latent Heat</b>	<b>Forest</b>	0.29	0.37	0.51	0.50
	<b>Alt Madlitz</b>	0.23	0.28	0.33	0.34
	<b>Conifer</b>	0.05	0.28	0.37	0.28
<b>Soil Moisture</b>	<b>Forest</b>	0.16	-0.29	0.03	0.15
	<b>Alt Madlitz</b>	0.41	0.11	-0.16	-0.04

### Supplementary Material 3: Temporal changes in water age estimations

All model resolutions showed a similar seasonal trend of water ages in layer 1 (Table S4), varying between the oldest water in spring and youngest water in the summer. The temporal variation changes consistently across the catchment, with the spatial variability of water ages shown on Fig. 7. Temporal trends of water ages in layer 2 were slightly different than layer 1 (Table S4), and revealed subtle but trivial differences between model resolutions. The oldest water was estimated in autumn and youngest water in the winter, a direct seasonal shift from layer 1.

70 **Table S4: Estimated seasonal water ages in soil layers 1 and 2, transpiration, and groundwater residence time for each model scale. Seasons are defined as winter (Dec – Feb), spring (Mar-May), summer (Jun – Aug), and autumn (Sep – Nov).**

	Season	Scale			
		250m	500m	750m	1000m
Layer 1 Age (days)	Winter	73 ± 16	58 ± 13	59 ± 12	62 ± 13
	Spring	93 ± 22	70 ± 18	72 ± 16	77 ± 17
	Summer	47 ± 14	29 ± 8	28 ± 8	28 ± 9
	Autumn	48 ± 12	35 ± 6	34 ± 6	33 ± 7
Layer 2 Age (days)	Winter	212 ± 192	159 ± 131	144 ± 112	165 ± 87
	Spring	219 ± 196	184 ± 143	175 ± 125	196 ± 87
	Summer	233 ± 196	181 ± 138	139 ± 126	190 ± 89
	Autumn	245 ± 191	178 ± 127	163 ± 115	186 ± 88
Transpiration Age (days)	Winter	147 ± 153	156 ± 158	180 ± 187	202 ± 213
	Spring	276 ± 236	296 ± 258	332 ± 280	357 ± 310
	Summer	335 ± 281	388 ± 357	453 ± 396	455 ± 397
	Autumn	305 ± 270	339 ± 351	390 ± 388	426 ± 374
Groundwater Mean Residence Time (years)	Winter	13.3 ± 8.0	21.4 ± 18.9	19.3 ± 18.4	23.5 ± 34.8
	Spring	13.3 ± 8.5	21.8 ± 19.6	18.4 ± 18.5	22.4 ± 33.4
	Summer	14.4 ± 8.7	23.3 ± 19.4	20.6 ± 18.9	24.2 ± 35.3
	Autumn	16.2 ± 9.6	27.2 ± 20.5	24.8 ± 20.3	26.4 ± 36.8

#### Supplementary Material 4: Calibrated rooting distribution

The rooting distributions in EcH<sub>2</sub>O(-iso) are defined using the depth of each soil layer and an exponential function (Kuppel et al., 2018) (single shape parameter, Root Distribution, Table S2). Lower values of the exponential parameter distribute roots more equally through all soil layers, while high values distribute more roots to near surface soil layers. Croplands and pasturelands were estimated to have a higher proportion of roots in the near surface soils for all model resolution (Fig. S4), despite a larger a priori root distribution range than conifers and broadleaves (Table S2). For the broadleaf and conifer forests, optimization of the root distribution showed more uniform distribution of roots with depth (note that layer 1 and 2 are much smaller volumes than layer 3).

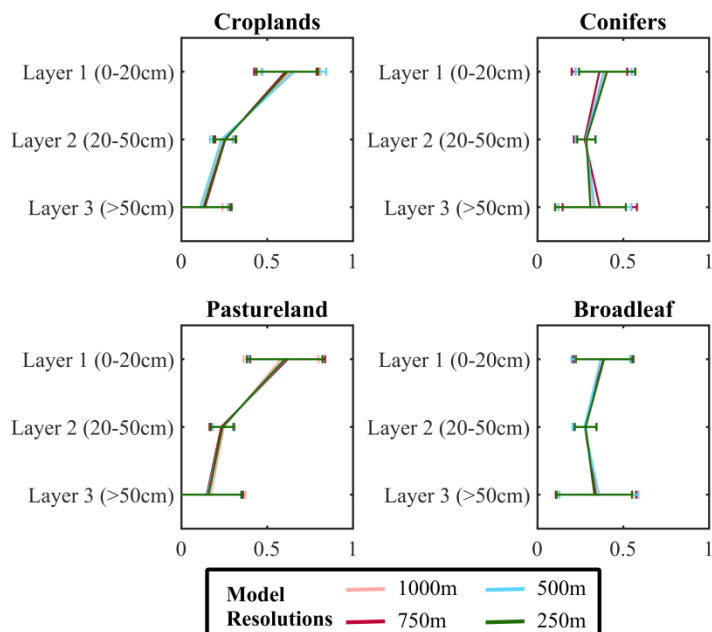


Figure S4: Estimated rooting profiles from the calibrated rooting distribution parameter.



## Supplementary Material 5: Correlation matrix of storage-flux-age-vegetation-soil

85 The correlation of primary fluxes; evapotranspiration (ET), soil evaporation (Es), transpiration (Tr), and groundwater  
 90 recharge (Re), primary storage; layer 1 (L1), layer 2 (L2), layer 3 (L3), and groundwater (GW), and primary storage and flux  
 95 ages; layer 1 (L1), layer 2 (L2), layer 3 (L3), and transpiration (Tr), is essential to understand how the catchment response  
 may change under varying conditions. Additionally, how the primary drivers of the fluxes, storage and water ages,  
 vegetation and soils are correlated across the catchment provides useful information for how management decisions may  
 affect the catchment hydrology and ecological growth. The annual sum of fluxes, annual average storage and water ages,  
 proportion of vegetation (cropland = Cr, broadleaf = BL, conifer = Co, and pastureland = Pa), and soil (brown earth = BE,  
 gley = GL, Peat = PE, and podzol = PZ) were spatially correlated with the Spearman rank correlation. The Spearman rank  
 correlation was used as it does not assume a normal distribution. Significance of the correlations was determined the 95th  
 percentile for all spatial locations up to the extent of the Demnitz Mill discharge location (Fig. 1a). Modelled fluxes,  
 storages, and ages outside this spatial domain were not considered. The colour-coded correlation matrix (Fig. S5) shows the  
 correlation for each age, storage, flux, vegetation, and soil relationship for each model resolution. Deep red colours indicate  
 strong positive correlation (e.g. storage in layers 1 and 2 to soil evaporation) while deep blue values indicate strong negative  
 correlation (e.g. all ages correlated to groundwater recharge). White squares indicate that no significant spatial correlation  
 was found.

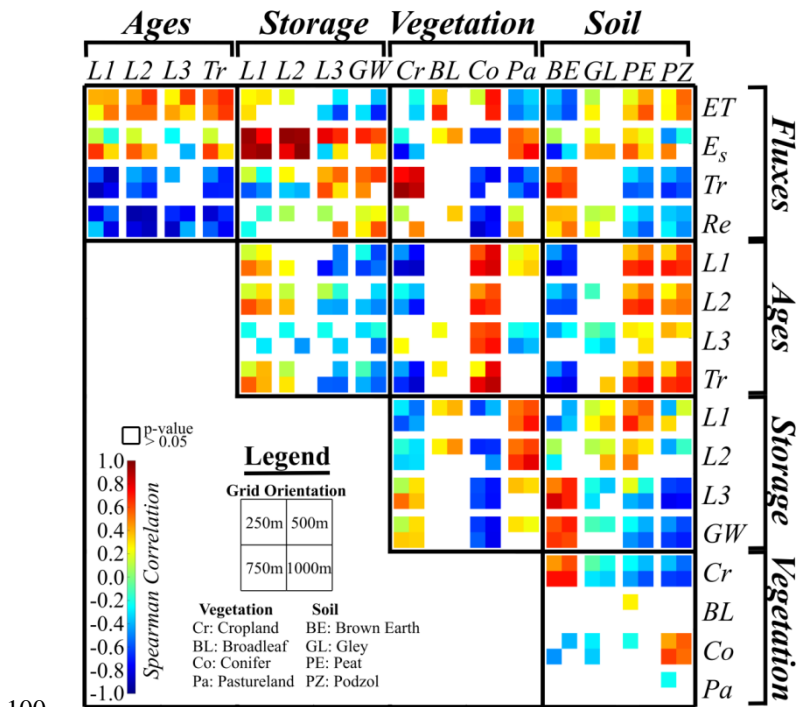


Figure S5: Spearman rank correlation matrix of flux-age-storage-vegetation-soil with annual average values (flux, and, and storage). No colours indicate that the correlations are insignificant to 95% threshold.

## References

- Ala-aho, P., Tetzlaff, D., McNamara, J. P., Laudon, H., and Soulsby, C.: Using isotopes to constrain water flux and age estimates in snow-influenced catchments using the STARR (Spatially distributed Tracer-Aided Rainfall–Runoff) model, *Hydrology and Earth System Sciences*, 21, 5089-5110, 10.5194/hess-21-5089-2017, 2017.
- Boyle, D. P., Gupta, H. V., and Sorooshian, S.: Toward improved calibration of hydrologic models: Combining the strengths of manual and automatic methods, *Water Resources Research*, 36, 3663-3674, 10.1029/2000wr900207, 2000.
- Douinot, A., Tetzlaff, D., Maneta, M., Kuppel, S., Schulte-Bisping, H., and Soulsby, C.: Ecohydrological modelling with EcH2O-iso to quantify forest and grassland effects on water partitioning and flux ages, *Hydrological Processes*, 10.1002/hyp.13480, 2019.
- Kleine, L., Tetzlaff, D., Smith, A., Wang, H., and Soulsby, C.: Using isotopes to understand evaporation, moisture stress and re-wetting in catchment forest and grassland soils of the summer drought of 2018, *Hydrol. Earth Syst. Sci. Discuss.*, 2020, 1-29, 10.5194/hess-2020-81, 2020.
- Kuppel, S., Tetzlaff, D., Maneta, M. P., and Soulsby, C.: EcH2O-iso 1.0: water isotopes and age tracking in a process-based, distributed ecohydrological model, *Geoscientific Model Development*, 11, 3045-3069, 10.5194/gmd-11-3045-2018, 2018.
- Smith, A., Tetzlaff, D., Kleine, L., Maneta, M. P., and Soulsby, C.: Isotope-aided modelling of ecohydrologic fluxes and water ages under mixed land use in Central Europe: The 2018 drought and its recovery, *Hydrological Processes*, 34, 3406-3425, 10.1002/hyp.13838, 2020.